POLITECNICO DI TORINO
Repository ISTITUZIONALE

Uncertainty Quantification of Geo-Magnetically Induced Currents in UHV Power Grid

(Article begins on next page)

20 April 2024

Uncertainty Quantification of Geo-magnetically Induced Currents in UHV Power Grid

Qing Liu, Yan-zhao Xie, *Member, IEEE*, Ning Dong, Yu-hao Chen, Min-zhou Liu, and Quan Li

Abstract—**Geo-magnetically induced currents (GICs) have attracted more attention since many EHV/UHV transmission lines have been built, or are going to be built in the world. However, when doing calculation of GICs based on the classical model, some input parameters, such as the earth conductivity and DC resistances of the grid, are uncertain or very hard to be determined in advance. Taking this into account, the uncertainty quantification model of the geo-electric fields and GICs is proposed in this paper. The uncertainty quantification of the maximums of the geo-electric fields and GICs during storms is carried out based on the Polynomial Chaos (PC) method. The results of the UHV grid, 1000 kV Sanhua Grid, were presented and compared to the Monte Carlo (MC) method. The total Sobol indices are calculated by using the PC expansion coefficients. The sensitivities of geo-electric fields and GICs to the input variables are analyzed based on the total Sobol indices. Results show that the GICs and geo-electric fields can be effectively simulated by the proposed model which may offer a better understanding of the sensitivities to input uncertain variables and further give a reasonable evaluation of the geomagnetic threat to the grid.**

Index Terms—**Geomagnetically Induced Currents, Polynomial Chaos, Uncertainty Quantification, Geo-electric fields, Total sobol indices**

I. INTRODUCTION

SOLAR activities, especially Coronal Mass Ejections (CMEs), solar flares and energetic particles, are the major factors that affect space weather and trigger geomagnetic disturbances (GMDs). The GMDs can induce low frequency currents into power networks, known as geo-magnetically induced currents (GICs) [1-3]. The GICs may cause half-cycle saturation in power transformers, produce harmonics, and increase reactive power demand and transformer spot heat. This can lead to serious problems, such as transformer damage, voltage dips, relay disoperation and system instability [4-6]. Although GMDs are more likely to happen in high latitudes, recently the phenomenon caused by GICs are also found in middle and low latitudes [7-8], such as South Africa, Brazil, and China, which attracts broad attention.

GIC calculation requires the induced geo-electric fields over the earth's surface. The "source" of this geo-electric field (i.e., the magnetosphere-ionosphere currents) can be approximately determined by an infinite line current, surface current or 3-dimensional current model. There are a number of methods based on different assumptions and simplifications that can be used to calculate the geo-electric fields and the GICs. A simple way is to apply an equivalent downward-propagating plane wave and assume that the earth is either uniform or layered [9]. A lot of work on geo-electric fields and GICs has been reported with specific parameters [10-15].

However, some input parameters are difficult to be precisely quantified, particularly in large scale power systems. For example, the earth conductivity along the depth of several hundred kilometers is an approximation of the actual structure due to the multiplicity on magnetotelluric inversion and noise interference [16]. Since the frequency of geo-electromagnetic variations is far less than that of electric power, the effect of geo-electric field can be regarded as a DC source. So the resistances play a dominant role for GIC calculation and the power grid can approximately be equivalent to a DC network [17]. For GIC calculation, the dynamic characteristics of AC voltages and transformer saturation should be taken into considered. As an engineering approach, nevertheless, to model the network as resistances is more acceptable. The DC resistances of transmission lines and the transformer windings should be regarded as variables due to their changes with temperatures and should be taken into consideration.

The ultra-high voltage power grid is the cornerstone of the smart grid in China and it is being developed at an unprecedented speed. Due to its small DC resistance and limited capability of UHV transformer to withstand DC bias, the UHV grid is more sensitive to geomagnetic hazards comparing to other grids.

In this paper, taking an UHV Grid in Sanhua China for example, we propose an efficient method based on the stochastic simulation tools of Polynomial Chaos (PC) to perform uncertainty quantification (UQ) for geo-electric fields and GICs. The earth conductivities and the DC resistances are used as input variables with proper distributions, and the output variables are the peak values of the time series of geo-electric fields and GICs during storm event. The results obtained give a clear indication of the GIC levels of all substations and the sensitivities of GICs in different substations to different input variables. The conclusions will provide comprehensive and useful information for GIC evaluation and mitigation.

II. UNCERTAINTY QUANTIFICATION MODEL OF THE GEO-ELECTRIC FIELDS AND GICs

A. Calculation Method of The Time Series of Geo-electric Fields and GIC

In GIC calculation, one-dimensional (1-D) earth model is mostly adopted due to its simplicity and acceptable accuracy. The variable conductivity of the earth can be modeled by a series of horizontal layers with specified conductivity and thickness. Based on the "plane wave" method, the surface impedance $Z_0(\omega)$ of m-layer earth can be calculated by using the recursive relation in [10]. In the frequency domain, $Z_0(\omega)$ is also the transfer function between the surface electric fields and magnetic field, the relationships between which are:

$$E_y(\omega) = -\frac{1}{\mu_0} B_x(\omega) Z_0(\sigma_1, \sigma_2, \ldots, \sigma_m, h_1, h_2, \ldots, h_{m-1}, \omega), \quad (1)$$

$$E_x(\omega) = \frac{1}{\mu_0} B_y(\omega) Z_0(\sigma_1, \sigma_2, \ldots, \sigma_m, h_1, h_2, \ldots, h_{m-1}, \omega). \quad (2)$$

where $\sigma_i (i=1,2,\cdots,m)$ and h_i ($i=1,2,\cdots,m$-1) are the conductivity and thickness of each layer, and ω is the angular frequency.

The real-time magnetic field data from magnetic observatory can be converted to frequency domain through Fourier transform. So the electric fields in frequency domain can be obtained by (1) and (2). Then by applying inverse Fourier transform, we can get the time series of $E_x(t)$ and $E_y(t)$. Due to the insignificant error, we ignore the effect of shield wires on geoelectric field calculation. These electric fields can be used as input to a power system model for every time increment to calculate the voltage sources, which drive GIC flows in power grid. For the transmission line from substation a to substation b, the voltage is given by

$$V_{ab}(t) = E_x(t) \cdot L_N + E_y(t) \cdot L_E. \quad (3)$$

where, L_N is the northward distance, and L_E is the eastward distance. They are related to the latitudes and longitudes of the two substations and can be calculated by the formulas in [18].

For the quasi-direct GIC, the power grid can be equalized as straightforward linear resistance network. Then GICs from substations to ground can be obtained by

$$GIC = (1+YZ)^{-1} J, \quad (4)$$

which is presented by Lehtinen and Pirjola [19], where, Y and Z are the network admittance matrix and the earthing impedance matrix, respectively. J depends on the voltages determined by the electric field along the transmission line and the line resistance, for example, for the node b, J_b is decided by

$$J_b = \sum_{b=1, b \neq a}^{N} \frac{V_{ba}}{R_{ba}}. \quad (5)$$

When the time series of geo-electric fields and GIC during a given storm event have been calculated, we can find the maximums of geo-electric fields and GIC during this storm event. The solving procedure can be presented in Fig. 1. The input variables are described by the n-dimensional vector ξ, which can be either the uncertain parameters of the layered earth or the DC resistances of the power grid. In this paper, what we are mainly concerned about, i.e. the output variables, are the maximums of the geo-electric fields and GICs during a storm event. For convenience, a function is used to represent the solving processing, and the output variables can be expressed by $y = Y(\xi_1, \xi_2, \ldots, \xi_n)$.
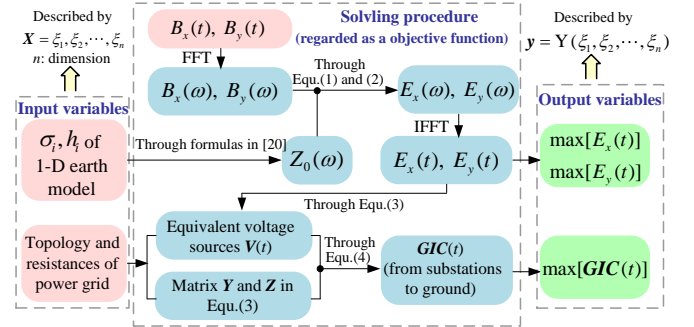

Fig. 1. Solving procedure of the maximums of geo-electric fields and GICs

B. Derivation of Polynomial Chaos Expansions for Output Variables

The traditional way to analyze the uncertainty of output variables in varied input scenarios is to use Monte Carlo (MC) method. The first step is to sample randomly according to the distribution type and intervals of the input variables. The samples are denoted by

$$\tilde{X}^{(s)} = (\tilde{\xi}_1^{(s)}, \tilde{\xi}_2^{(s)}, \cdots, \tilde{\xi}_n^{(s)}) \quad s = 1, 2, \ldots, m. \quad (6)$$

The sample number (i.e. m) usually should be big enough to obtain satisfactory results and in this paper m is set to be 10,000. Next, put the samples into the objective function, then the outputs for all different sample sets can be calculated.

Although MC method is simple and clear, its efficiency decreases with the increasing of the sample number. Some techniques can solve this problem very well [20-21], such as PC method. According to PC theory, the objective function can be expanded with respect to X using a series of orthogonal basis functions. In practical, we need to truncate the order of expansion to a finite order P. After truncation, the expansion can approximate the real response.

$$Y(X) \approx \hat{Y}(X) = \sum_{k=0}^{P} A_k \Psi_k(X). \quad (7)$$

where, A_k represent the expansion coefficients to be estimated, $\Psi_k(X)$ is a class of multivariate polynomials which involve products of the one-dimensional polynomials; k is the term

number of the expansion. To obtain the expansion, multivariate polynomials and the coefficients need to be determined.

1) *Determination of Multivariate Polynomials*

For each input variable, its one-dimensional orthogonal polynomial basis $\psi_j(\xi_i)$ of j-order can be determined by Askey scheme [22]. Then $\Psi_k(X)$ can be obtained easily by multiplying $\psi_j(\xi_i)$. Traditionally, the PC expansion includes a complete basis of polynomials up to a fixed total-order. For example, the multidimensional polynomials for a 2-order expansion over two random dimensions are

$$
\begin{aligned}
\Psi_0(\xi_1,\xi_2) &= \psi_0(\xi_1)\psi_0(\xi_2), \quad \Psi_1(\xi_1,\xi_2) = \psi_1(\xi_1)\psi_0(\xi_2) \\
\Psi_2(\xi_1,\xi_2) &= \psi_0(\xi_1)\psi_1(\xi_2), \quad \Psi_3(\xi_1,\xi_2) = \psi_2(\xi_1)\psi_0(\xi_2) \\
\Psi_4(\xi_1,\xi_2) &= \psi_1(\xi_1)\psi_1(\xi_2), \quad \Psi_5(\xi_1,\xi_2) = \psi_0(\xi_1)\psi_2(\xi_2)
\end{aligned} \quad (8)
$$

Regarding to total-order expansion method (truncating all the product items of one-dimensional polynomials to d-order), the number of the coefficients, i.e. the total number of the expansion terms should be given by

$$
Q = P + 1 = (n+d)! / (n! d!). \quad (9)
$$

2) *Calculation of Polynomials Coefficients*

For one-dimensional input variable, the coefficients can be calculated by numerical integration. But for multi-dimensional input variables, numerical integration is no longer efficient. We use stochastic response surface method to calculate the coefficients. The first step is to sample randomly from the parameter space of the input variables, which is denoted by

$$
\{\tilde{X}^{(s')}, \ s'=1,2,\cdots L\}, \text{ where:} \tilde{X}^{(s')} = \tilde{\xi}_1^{(s')}, \tilde{\xi}_2^{(s')},\cdots,\tilde{\xi}_n^{(s')}. \quad (10)
$$

To achieve the acceptable accuracy, the number of sample sets (i.e. L) used to solve the coefficients usually should be no less than $2Q$.

The second step is to plug these L sets of samples into the objective functions $Y(X)$ and the right-hand side of (7) respectively, and then L real responses and L approximate responses can be obtained. The coefficients should make the approximations close to the real ones, which can be written by L equations expressed in matrix equation

$$
\begin{bmatrix}
\Psi_0(\tilde{X}^{(1)}) & \Psi_1(\tilde{X}^{(1)}) & \cdots & \Psi_P(\tilde{X}^{(1)}) \\
\Psi_0(\tilde{X}^{(2)}) & \Psi_1(\tilde{X}^{(2)}) & \cdots & \Psi_P(\tilde{X}^{(2)}) \\
\vdots & \vdots & \ddots & \vdots \\
\Psi_0(\tilde{X}^{(L)}) & \Psi_1(\tilde{X}^{(L)}) & \cdots & \Psi_P(\tilde{X}^{(L)})
\end{bmatrix}
\begin{bmatrix}
A_0 \\ A_1 \\ \vdots \\ A_P
\end{bmatrix}
=
\begin{bmatrix}
Y(\tilde{X}^{(1)}) \\ Y(\tilde{X}^{(2)}) \\ \vdots \\ Y(\tilde{X}^{(L)})
\end{bmatrix}. \quad (11)
$$

Equation (11) can be simplified as:

$$
\mathbf{BA} = \mathbf{Y} \quad (12)
$$

Obviously, Equation (11) is an overdetermined equation, and the coefficients are the solution of this equation. If matrix $\mathbf{B}^{\mathrm{T}}\mathbf{B}$ is nonsingular, Equation (11) has a unique solution, which can be calculated by (13) according to least quadratic regression.

$$
\hat{\mathbf{A}} = (\mathbf{B}^{\mathrm{T}}\mathbf{B})^{-1}\mathbf{B}^{\mathrm{T}}\mathbf{Y} \quad (13)
$$

The workflow of PC method is shown in Fig. 2. Once the coefficients are obtained, the PC expansions regarded as surrogate models of the objective function $Y(X)$ are obtained.

Obviously, to get the PC expansions for output variables it only needs a few iterations to solve the objective function. Then, we can carry out uncertainty quantification with these surrogate models available, which is much faster than running a large number of MC simulations for the objective function.
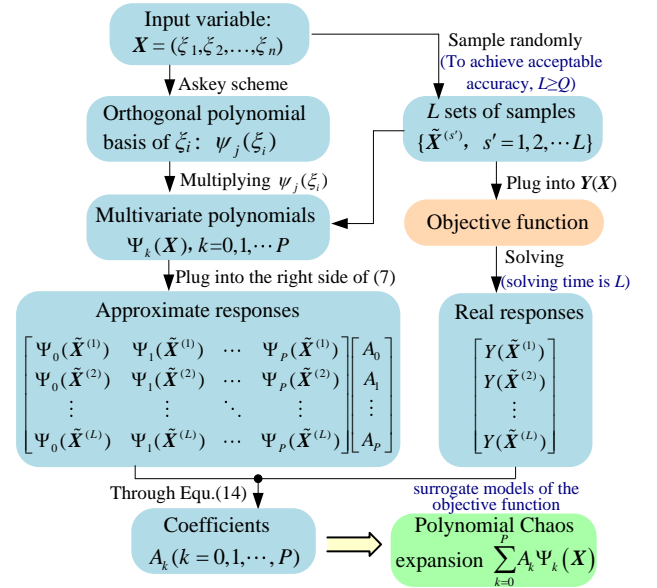

Fig. 2. The workflow of the PC method

III. Uncertainty Quantification of Geo-electric fields and GICs of Sanhua Grid

A. Topology and Parameters of Sanhua Grid

Sanhua Grid is an UHV AC system in China, interconnecting 3 regional power grids including North China grid, Central China grid and East China grid. Fig. 3 shows the geographic location of the Sanhua Grid discussed in this paper, within which only the level of 1000kV is considered. The grid consists of 37 substations at 1000 kV and 45 AC transmission lines. The substations are numbered from 1 to 37, and their numbers and names are all labeled in Fig. 3. The transmission lines are labeled with blue numbers.

Calculation of GIC requires three sets of resistance parameters. The typical value of substation grounding resistance is 0.1Ω, assuming all transformers grounded directly. The 1000 kV lines are comprised of 8-bundled conductors LGJ-500/35 per phase, and the DC resistance of every phase is 0.0095 Ω/km (at 20°C), the lengths of which can be obtained from electric power design institutes. From transformer manufacturers, the typical values of DC resistance per phase of

series and common winding are 182.7 mΩ and 141.5 mΩ at 75 ℃, respectively. With these parameters the equivalent circuit of this grid can be modeled.
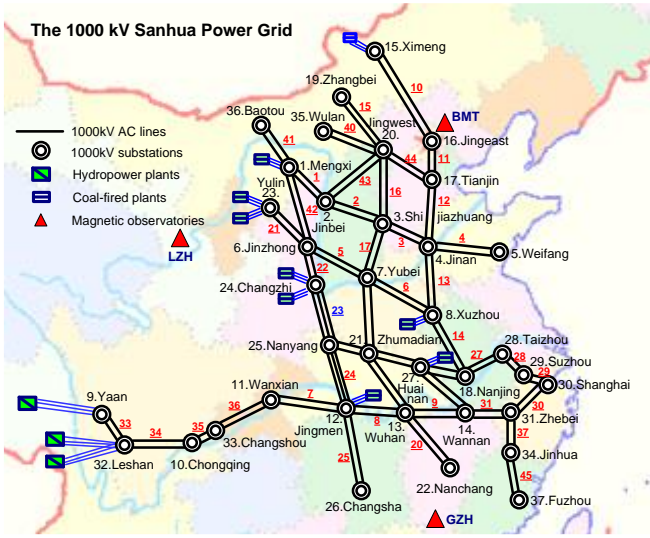

Fig. 3. Geographic location of the part of Sanhua 1000kV power grid considered in this paper.

In this section, we will carry out uncertainty quantification for the maximums of geo-electric fields and GICs during a storm event. As an example, a GMD event on the 7-8 November, 2004 was selected. The magnetic field recordings from three main magnetic observatories (marked by the red triangles in Fig. 3) starting from November 7 until the end of November 8 are obtained, which comprised 2880 data points with a sampling interval of 1 minute. Magnetic derivatives against time (dB/dt) were calculated from the magnetic field recordings that are shown in Fig. 4. It shows that the rates of magnetic field change at three observatories are almost identical. Therefore, it is reasonable and acceptable to assume the magnetic field to be uniform over the geographical area of the entire power grid. In the next calculation, the magnetic field records from BMT observatories will be used.

Based on the 4-layer earth conductivity model [23] and the interpretation of past geophysical measurements [24-25], the ranges of the soil layer conductivities are roughly determined and their values are assumed to be uniform distribution. Nevertheless, the uniform distribution may not be optimal, if sufficient values of soil conductivities can be acquired, then more preferable distribution would be inferred based on Bayesian methods. Subscripts 1-4 are used to denote each layer from the top layer downwards. The thicknesses of the top three layers are 30km, 60km, and 60km. The resistivity variable ranges assigned to each layer are [100, 2000] Ω-m, [50, 770] Ω-m, and [25, 2000] Ω-m. Under the depth of 150 km, it is a bottom half space with the resistivity from 1Ω-mto 3 Ω-m.

B. UQ for the Maximums of Geo-electric Fields

For geo-electric fields study, the 4 dimensional input variables are the conductivities of the 4-layer earth following random distribution in their respective variable ranges. They are denoted by $X = (\xi_1, \xi_2, \xi_3, \xi_4) = (\sigma_1, \sigma_2, \sigma_3, \sigma_4)$.

According to the distribution characteristic of input variables, 10,000 samples can be obtained and used as 10,000 input conditions. Then 10,000 outputs can be calculated either by MC method or by PC method. With these results, we can calculate the mean, the standard deviation and the median of geo-electric field maximums. Taking the results of MC method as a reference, we can calculate the error percentages between PC method and MC method. For PC method, different truncation orders have different calculation accuracies. The error percentages between two methods with different orders are compared in Table I.
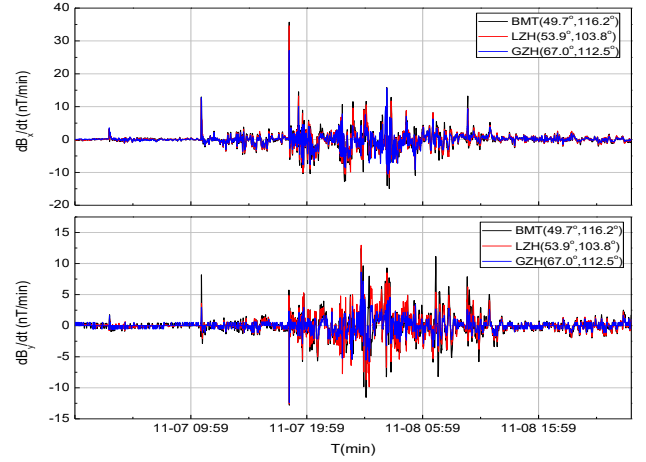

Fig. 4. The dB/dt calculated from recorded magnetic-field variations at three magnetic observatories, November7-8, 2004.

TABLE I
EFFECT OF TRUNCATION ORDER OF PC METHOD ON ERROR PERCENTAGE

d	Mean (%)		Standard deviation(%)		Median (%)		Q	L
	E_x	E_y	E_x	E_y	E_x	E_y		
1	5.288	0.378	23.83	14.07	10.30	2.459	5	10
2	0.261	0.012	2.627	2.382	0.476	0.016	15	30
3	0.027	0.154	2.628	3.940	0.689	0.202	35	70
4	0.061	0.013	0.390	0.767	0.071	0.129	66	132
5	0.034	0.073	0.496	1.650	0.018	0.021	126	252

Here, d is the truncation order of the PC expansions. Q is the number of polynomial terms. When we calculate the coefficients of PC expansion, we sample L(equal to 2Q) sets of samples and put them into the objective functions. So L is also the solution times to the objective function.

It indicates that the higher the order is, the more accurate the results are. Considering that the term number and the solution time will increase along with the orders, the 3rd order PC expansion would be appropriate. Compared with 10,000 iterations to the objective function of MC method, the 3rd order PC method only needs to solve the objective function 70 iterations to achieve approximated accuracy.

The cumulative probability density (CDF) curves of the maximums of E_x and E_y are shown in Fig.5, which provides the ranges of geo-electric fields maximums during the storm event and the probabilities of different maximums.

C. UQ for the Maximums of GIC

The DC resistances of transmission lines and transformer windings given above are the values under the condition of 20 ℃. In practical, they would change with temperatures. In addition, the product parameters of different manufacturers

may be slightly different. The grounding resistance may change with soil moisture and corrosion situations of the grounding conductor. Hence, for the uncertainty quantification of GIC, DC resistances should be treated as input variables as well. The input variables are therefore seven-dimensional, which can be expressed by the vector of $X = (\sigma_1, \sigma_2, \sigma_3, \sigma_4, R_1, R_2, R_3)$. Here, R_1 denotes the resistance per unit length of transmission line, R_2 denotes the winding resistance, and R_3 denotes the substation grounding resistance of the. Considering the practical operation, we roughly assume that the transmission line resistances vary from 0.00912 Ω/km to 0.0114 Ω/km, and the values of transformer windings range between ±8%. Considering the design requirement of grounding resistance and the practical operation in UHV substations, the reasonable range of grounding resistance is from 0.08 Ω to 0.12 Ω. The resistance values are assumed to follow uniform distribution.
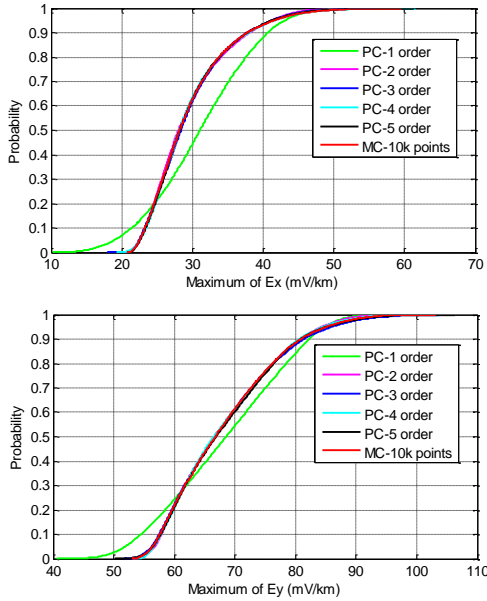

Fig. 5. Compare of CDF of the geo-electric fields maximums obtained by PC method and MC method.
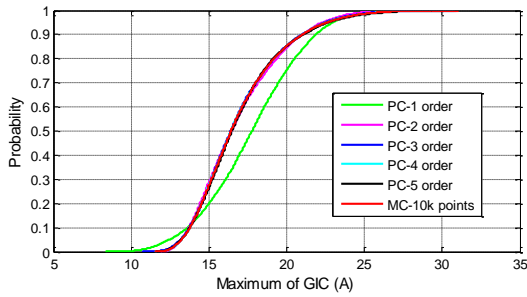

Fig. 6. Comparison of CDF curves of GIC maximums in No.1 substation calculated by PC expansions and MC method

Similarly, the GIC maximums of all substations in Sanhua grid can be obtained by using the PC method. For example, the CDF curves of the No.1 substation computed by MC method and PC method under different orders are shown in Fig.6. It shows that the accuracy is acceptable when the order is greater than two. The same conclusion could be derived from other substations.

The number of polynomial terms and program running time under different orders are compared in Table II. For MC method, it takes 3h 26min to finish 10,000 outputs. But even for 5-order PC expansion including 792 polynomial terms, it would take only about half an hour to get 10,000 outputs. Obviously, PC method can greatly shorten simulation time and increase the computation efficiency.

TABLE II
COMPARISONS OF PC METHOD UNDER DIFFERENT ORDER

Order	1	2	3	4	5
Q	8	36	120	330	792
L	16	72	240	660	1584
t_1	40.068s	93.654s	4min39s	14min5s	32min24s
t_2	4.404s	5.630s	11.932s	34.196s	109.844s

Q and L have the same meaning as those in Table I. Here t_1 is the approximate program run time to get the PC expansions, and t_2 is the program run time to substitute 10,000 sample sets in the PC expansion to obtain 10,000 outputs. The main computer configuration is 8G memory and Intel i5-5200U CPU (2.2GHz).

After comprehensive comparison, we choose the 3-order PC expansions to carry out uncertainty quantification for GIC maximums. Then we carry out statistical analysis for the 10,000 outputs to get extra information, such as variances, means, and cumulative probability density. The results are shown in Fig.7, which provides the GIC maximums in all the 37 substations, as well as their interval distributions. It shows that in almost half of the 37 substations, the maximums of GIC from substation to the earth would exceed 20 amperes. Especially, the GIC in the Jingwest substation and the Shanghai substation are larger than the others, which can be explained by the "edge effect".

Similarly, the CDF of all output variables could be calculated. Due to limited space, only the CDF curves and histograms of 12 crucial substations are listed in Fig. 8. The information provided by Fig. 8 could clarify the distribution characteristics of GIC maximums and how frequently the values may occur.

Obviously, for each input sample, there is a corresponding output. And among these outputs, we can find the condition under which the highest GIC maximums would appear. For example, GIC time series in three substations are shown in Fig. 9. The horizontal coordinate donates the time with the unit of minutes. The red texts are the values of GIC maximums during this storm event.

IV. SENSITIVITIES STUDY

The sensitivity analysis based on Variance Decomposition can be used to quantify the influence of the input variables on the output variables.

The variance of the objective function and the partial variances of single input variable or between input variables are denoted by V and $V_{i1,i2,...is}$, respectively. The *Sobol indices* S_i and the *total Sobol indices* S_i^T of the response $Y(X)$ with respect to the input variables x_i are as follows[26]:

$$S_{i_1,\cdots,i_s} = \frac{V_{i_1,\cdots,i_s}}{V} \quad 1 \le i_1 < \cdots < i_s \le n;\ s = 1,2,\cdots,n, \quad (15)$$

$$S_i^T = \sum_{\tau_i} S_{i_1, \cdots, i_s}, \ \tau_i = \{(i_1, \cdots, i_s) : \exists k, 1 \le k \le s, i_k = i\}. \quad (16)$$

For d-order PC expansion, the *total Sobol indices* can be estimated by

$$S_i^T = \frac{\sum_{\gamma_i} A_{i_1, \cdots, i_t}^2}{V}, \ \gamma_i = \{(i_1, \cdots, i_t) : \exists k, 1 \le k \le t, i_k = i\} \quad (17)$$

$$1 \le i_1 < \cdots < i_t \le n; \ t = 1, 2, \cdots, d. \ V = \sum_{i_1=1}^{n} A_{i_1}^2 + \sum_{i_1=1}^{n} \cdots \sum_{i_d=1}^{i_{(d-1)}} A_{i_1, i_2, \cdots i_d}^2$$

In order to illustrate the effects of all input random variables

mentioned previously on the output variables, we calculate the *total Sobol indices* with the coefficients solved above. The *total Sobol indices* of the maximums of geo-electric fields to the earth conductivities are presented in Fig. 10.

Regarding to the example studied in this paper, it shows that the northward field is mainly related to the conductivities of the top two layers, and the eastward field is more sensitive to the conductivity of the second layer. The earth conductivity below 150 km has little effect on geo-electric fields.
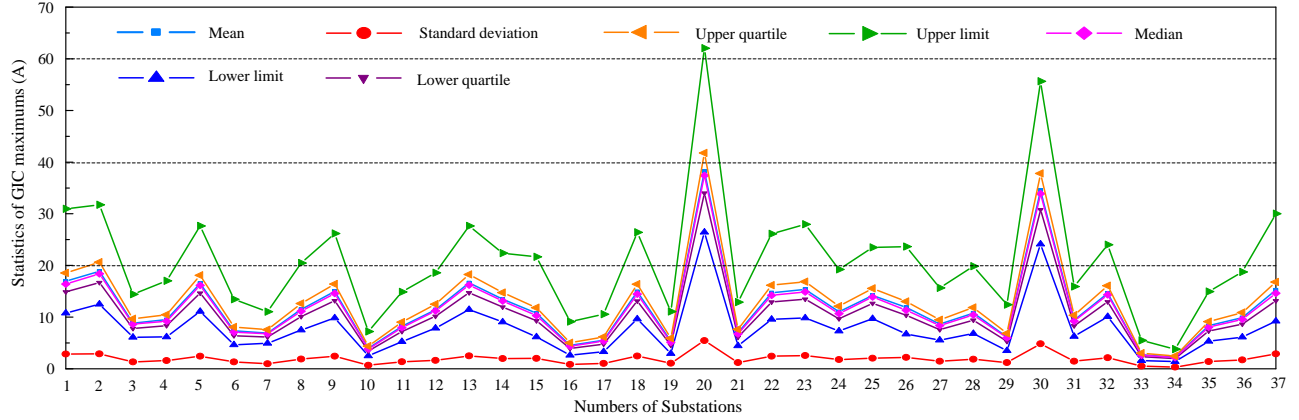

Fig. 7. Comparison of seven kinds of statistic parameters of GIC maximums in 37 substations.
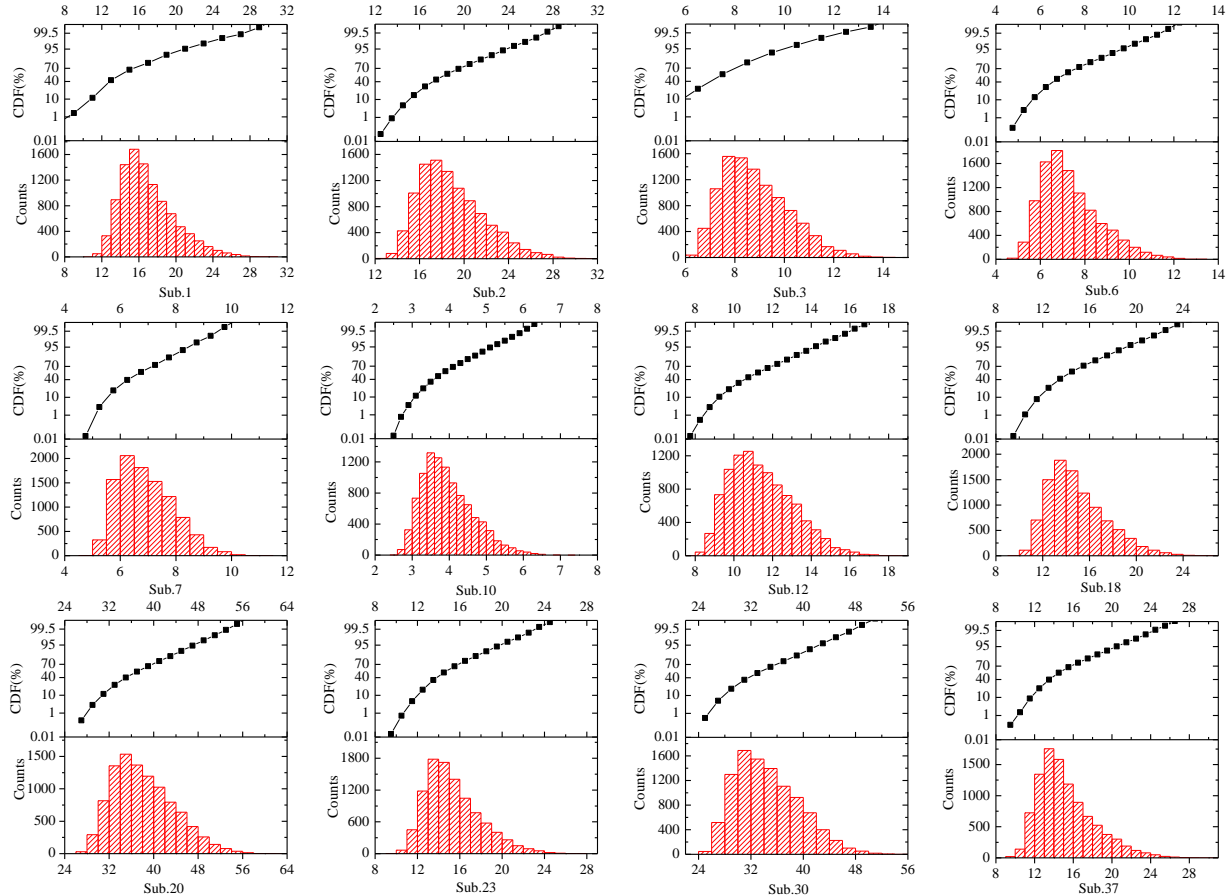

Fig. 8. Cumulative probability density curves and histograms of 12 crucial substations
The horizontal axis denotes the maximum of GIC with the unit of ampere. The numbers of substations are labeled below the graph.
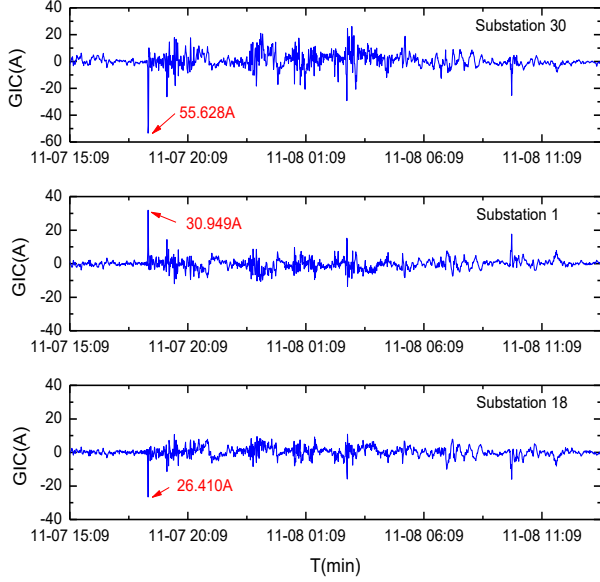
Fig. 9. The time series of GICs in three substations

The same work can be done for the GICs from substation to the ground. In Fig. 11, for the given distribution characteristics of the input variables in this paper, we list the *total Sobol indices* of the 12 substations considered in section III. Obviously, the GIC maximums are more sensitive to earth conductivities than the resistances, especially to the conductivity of the second layer. The influence of the 7 dimensional input variables on different substations is mainly due to their different geographic locations as well as their relative positions within the grid.

V. CONCLUSIONS

In this paper, considering the complex and uncertain of the input parameters in GIC calculation, we propose an uncertainty quantification model of the geo-electric fields and GICs. The uncertainty quantification for the geo-electric fields and GICs of a UHV power grid is carried out.

The PC expansion provides an efficient surrogate model to replace the objective function which can be used to analyze the uncertainty of the origin problem easily. For the calculation of GIC under 10,000 sample sets, the computational time of the PC method takes only one fortieth of that of the MC method.

For the considered storm event, the northward fields and eastward fields vary from 18.654 mV/km to 55.791 mV/km, and from 51.864 mV/km to 103.416 mV/km, respectively. In all the substations within the grid, 17 stations experience GICs exceeding 20 amperes in amplitude. GIC levels of some substations are rather threatening, especially in substations No.20 and No.30.

The *total Sobol indices* are calculated by using the PC expansion coefficients. Sensitivity analysis shows that, for the given earth model, the conductivity of the second layer has a greater impact on the geo-electric fields and GICs than the other layers. In different substations, the GICs are sensitive to their geological locations involving the seven dimensional input variables. Sufficient consideration should be given to the

grounding resistance of substations when carrying out GIC evaluation and mitigation.

The proposed method can effectively offer a better understanding of the sensitivities of GICs to input uncertain variables and give a reasonable evaluation of the geomagnetic hazards to power system. In the future, we will strive to acquire more information to set up exact earth conductivity model for GIC uncertainty quantification. Furthermore, we will monitor the substations where the GIC levels are relatively high in order to validate the computational model that makes it possible to provide predicted GIC based on the correlative predicted data of space weather.
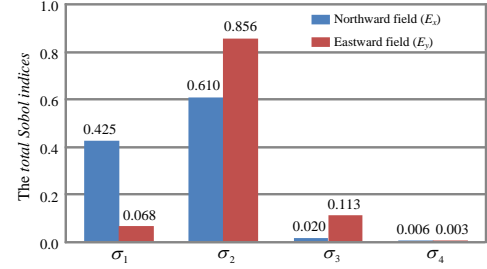

Fig. 10. The *total Sobol indices* of the maximums of geo-electric fields σ_1, σ_2, σ_3, and σ_4 are the earth conductivities of the 4-layer model, respectively.

Fig. 11. The *total Sobol indices* of the maximums of GICs in 12 substations. σ_1, σ_2, σ_3, and σ_4 are the earth conductivities of the 4-layer model. R_1 denotes the resistance per unit length of transmission line; R_2 denotes the winding resistance.

VI. ACKNOWLEDGEMENT

REFERENCES

[1] D. H. Boteler, R. Pirjola, and H. Nevanlinna, "The effects of geomagnetic disturbances on electrical systems at the Earth's surface," *Adv. Space Res.*, vol. 22, no. 1, pp. 17–27, Sep. 1998.

[2] R. Pirjola, "Geomagnetically Induced Currents During Magnetic Storms," *IEEE Trans. Plasma Science*., vol. 28, no. 6, pp. 1867-1873, Dec. 2000.

[3] Bolduc, L, P. Langlois, D. Boteler, "A study of geoelectromagnetic disturbances in Québec, 2. Detailed Analysis of a Large Event," *IEEE Trans. Power Del*., vol. 15, no. 1, pp. 272-278, Feb. 2000.

[4] D. Boteler, R. Pirjola, Ari Viljanen, and Olaf Amm, "Prediction of Geomagnetically Induced Currents in Power Transmission System," *Adv. Space Res*., vol. 26, no. 1, pp. 5-14, Mar. 2000.

[5] Vera V. Vakhnina, Vladimir A. Shapovalov, Vladimir N. Kuznetsov, and Dmitry A. Kretov, "The Influence of Geomagnetic Storms on Thermal Processes in the Tank of a Power Transformer," *IEEE Trans. Power Del*., vol. 30, no. 4, pp. 1702-1707, Aug. 2015.

[6] W.A. Radasky, "Impacts of variations of geomagnetic storm disturbances on high voltage power systems," *IEEJ Trans. Power & Energy*., vol. 133, no. 12, pp. 931-934, Dec. 2013.

[7] CDS Barbosa, GA Hartmann, KJ Pinheiro, "Numerical modeling of geomagnetically induced currents in a Brazilian transmission line," *Advances in Space Research*., vol. 55, no. 4, pp. 1168-1179, Nov. 2015.

[8] Q. Liu, K. Han, and Y. Bai, "Analysis of distribution regularities and sensitivity of geomagnetically induced currents in planned Xinjiang 750kV power grid," *Power System Technology*., vol. 41, no. 17, pp. 3678-3684, Nov. 2017.

[9] Pirjola. R., "Review on the calculation of surface electric and magnetic fields and of GICs in ground based technological systems," *Surveys in Geophysics*, vol. 23, no. 1, pp. 71-90, Jan. 2002.

[10] D. Boteler, "The use of linear superposition in modelling geomagnetically induced currents," in Proc .*IEEE Power & Energy Society General Meeting (PES)*, 2013, pp. 1-5.

[11] D. H. Boteler, "The Evolution of Québec Earth Models Used to Model Geomagnetically Induced Currents," *IEEE Trans. Power Del*., vol. 30, no. 5, pp. 2171-2178, Oct. 2015..

[12] L. Marti, C. Yiu, A. Rezaei-Zare, and D. Boteler, "Simulation of Geomagnetically Induced Currents With Piecewise Layered-Earth Models," *IEEE Trans. Power Del*., vol. 29, no. 4, pp. 1886-1893, Aug. 2014.

[13] Gilbert, J. L, "Simplified Techniques for Treating the Ocean-Land Interface for Geomagnetically Induced Electric Fields," *IEEE Trans. Electromagn Compat*., vol. 57, no. 4, pp. 688-692, Aug. 2015

[14] Love, J. J., Lucas, G. M., Kelbert, A and Bedrosian, P. A. "Geoelectric Hazard Maps for the Mid-Atlantic United States: 100 Year Extreme Values and the 1989 Magnetic Storm," *Geophysical Research Letters*, vol. 45, no. 1, pp. 5-14, Jan. 2018.

[15] H. Karami , K. Sheshyekani , A. Rezaei-Zare , et al. "Effect of Mixed Propagation Path on Electromagnetic Fields at Ground Surface Produced by Electrojet," *IEEE Trans. Electromagn Compat*., vol. 60, no. 6, pp. 2019-2024, Dec. 2018.

[16] Chen X B, Lu Q T, Zhang K, "Review of magnetotelluric data inversion methods," *Progress in Geophys*., vol. 26, no. 5, pp. 1607-1619, Oct. 2011.

[17] Albertson, V. D, Kappenman, J. G, N. Mohan, "Load-Flow Studies in the Presence of Geomagnetically-Induced Currents," *IEEE Trans. on Power Apparatus & Systems*., vol. PAS-100, no. 2, pp. 594-607, Feb. 1981.

[18] R. Horton, D. Boteler, T. J. Overbye, R. Pirjola, and R. C. Dugan, "A test case for the calculation of Geomagnetically Induced Currents," *IEEE Trans. Power Del*., vol. 27, no. 4, pp. 2368-2373, Oct. 2012.

[19] M. Lehtinen, and R. Pirjola, "Currents produced in earthed conductor networks by geomagnetically induced electric fields," *Annales Geophysicae*., vol. 3, no. 4, pp. 479-484, Jan. 1985.

[20] Z. Fei, Y. Huang, J. Zhou, and Q. Xu, "Uncertainty quantification of crosstalk using stochastic reduced order models," *IEEE Trans. Electromagn. Compat*., vol. 59, no. 1, pp. 228-239, Feb. 2017.

[21] S. Oladyshkin, and W. Nowak, "Data-driven uncertainty quantification using the arbitrary polynomial chaos expansion," *Reliability Engineering & System Safety*., vol. 106, no. 4, pp. 179-190, May. 2012.

[22] Xiu. D, and G. E. Karniadakis, "The Wiener-Askey Polynomial Chaos for Stochastic Differential Equations," *SIAM Journal on Scientific Computing*., vol. 24, no. 2, pp. 619-644, Oct. 2002.

[23] K. Zheng, "Reaaarch on Influence Factors and Modelling Methods of Geomagnetically Induced currents in Large Power Grid," Ph.D. dissertation, North China Electrical Power University., China, 2014.

[24] W. Wei, G. Ye, et al. "Geoelectric structure of lithosphere beneath eastern North China: features of a thinned lithosphere from magnetotelluric soundings," *Earth Science Frontiers*, vol. 15, no. 4, pp. 204-216, Jul. 2008.

[25] Y. Liu, Y. Xu. "Lithospheric electrical characteristic in South China and its geodynamic implication," *Chinese J. Geophys*., vol. 56, no. 12, pp. 204-216, Dec. 2013.

[26] I. M. Sobol, "Global sensitivity indices for nonlinear mathematical models and their Monte Carlo estimates." *Mathematics and Computers in Simulation*., vol. 55, no. 1-3, pp. 271-280, Feb. 2001.

Qing Liu was born in in 1978. She received the B.Sc. degree and M.S.degree in electrical engineering from Chongqing University in 2000 and Xi'an Jiaotong University in 2005. She is currently working toward the Ph.D degree in electrical engineering in Xi'an Jiaotong University. She is also an associate professor in Xi'an University of Science and Technology. Her research interest includes modeling and assessing geomagnetically induced currents in the power grid.

Yan-zhao XIE was born in in 1973. He received the Ph.D. degree in electrical engineering from Tsinghua University, China, in December, 2005. He is currently a Professor of Xi'an Jiaotong University, China. His research interests include electromagnetic transients in power system, electromagnetic compatibility etc. He has been the director of National Center for International Research on Transient Electromagnetics and Applications since 2016.

Yu-hao Chen received the B.Sc. degree in electrical engineering from Xi'an Jiaotong University, Xi'an, China, in 2015, where he is currently pursing the Ph.D. degree in electrical engineering. His research interest is effect evaluation of electromagnetic environments.

Ning Dong received the B.Sc. degree in electrical engineering department from Xi'an Jiaotong University in 2016. She is currently a PhD candidate in Xi'an Jiaotong University. Her research interest is modeling and uncertainty quantification of multiconductor transmission lines coupling.

Min-zhou Liu received the B.Sc. degree in electrical engineering from Xi'an Jiaotong University in 2017, where he is currently working toward the M.S. degree. His research interests include effects evaluation of electromagnetic environments and reliability evaluation of power system.

Quan Li is a Tenure Lecturer at the University of Edinburgh, Fellow of Higher Education Academy, and Theme Leader of Applied Superconductivity. He focuses on electromagnetism and superconducting applications in Energy and Healthcare sectors.